FEASIBILITY STUDY OF PARAFFIN-BASED FUELS FOR HYBRID ROCKET ENGINE APPLICATIONS

Elena Toson,[1,*] Mario Kobald,[2] Emanuele Cavanna,[1] Luigi T. De Luca,[1] Giovanni Consolati,[1] & Helmut Ciezki[2]

[1] *Space Propulsion Laboratory, Aerospace Engineering Dept., Politecnico di Milano, I-20156 Milan, MI, Italy*

[2] *Institute of Space Propulsion, DLR – German Aerospace Center, D-74239 Hardthausen, Germany*

[*] Address all correspondence to Elena Toson E-mail: elena.toson@polimi.it

1. INTRODUCTION

Hybrid rocket engines offer some known advantages with respect to both solid and liquid systems, based upon the work of De Luca (2009) and Altman and Holzman (2007). Hybrid rockets are known for their intrinsic safety because the oxidizer and fuel are stored in separated tanks. Furthermore, there are multiple advantages, such as an overall system simplicity, the capability for multiple on-and-off operations by opening and closing the oxidizer's main valve, and the possibility of controlling the oxidizer-to-fuel mixture ratio by throttling the oxidizer mass flow rate. Finally, there is an increased

NOMENCLATURE

$E_{r,\text{av}}$	averaged elastic modulus, MPa (psi)	ρ	density, kg/m^3 (lb/inch^3)
		σ_r	maximum stress, MPa (psi)
r_f	regression rate, mm/s		
$r_{f,\text{HTPB}}$	regression rate for HTPB-based mixtures, mm/s		**Abbreviations**
		AS	stearic acid
$r_{f,\text{wax}}$	regression rate for wax-based mixtures, mm/s	CP	congealing point
		DP	dropping point
		DSC	differential scanning calorimetry
	Greek symbols		
γ	shear rate, s^{-1} (s^{-1})	El	elongation
η	dynamic viscosity, Pa s (psi/s)	G	graphite
λ	linear thermal expansion coefficient, K^{-1} (F)	OilC	oil content
		SD	standard deviation
ν	Kinematic viscosity, Pa s (psi/s)	SP	solidification point

flexibility on the solid fuel/oxidizer selection that can reduce the environmental impact. Reduced development and recurring costs for hybrid rockets are expected with respect to solid rocket motors and liquid rocket engines. Hybrid rocket development began in 1932 with the Soviet GIRD-9 LO2/gelified gasoline motor, but extensive research on hybrids started in 1960s. The most famous example of hybrid engine development is the hybrid motor developed in 2003 by Scale Composites and SpaceDev for the suborbital vehicle SpaceShipOne, based on N_2O/hydroxy-terminated polybutadiene (HTPB). The main drawback and reason for delayed development of hybrid technology, with respect to liquid and solid ones, is the low regression rate of the fuel that does not allow high fuel loading and high thrust densities, resulting in a complex multiport grain design, as discussed by Boardman (2001) and De Luca (2009). This solution inevitably causes the formation of large amounts of residuals and the need for a web support structure. It also compromises the grain structural integrity and requires a precombustion chamber or individual injectors for each port. Different approaches have been studied and are under study. Some techniques, such as the addition of oxidizing agents, metal particles, and the swirl injection for increasing local mass flux, are based upon the enhancement of heat-transfer rates to the fuel surface. One approach is based on the use of ingredients that melt at the regression surface. As theorized by Karabeyoglu et al. (2002a, 2002b), the melted layer liquid droplets are believed to be entrained by liquid layer instabilities, thus bringing an additional term in the regression rate empirical law. This implies that the total fuel regression rate is a combination of fuel vaporization rates from its surface and the fuel mass loss by droplet entrainment. This corresponds to the reduction of the

heating rate requirement to the evaporating fuel for the same amount of mass loss from the bulk fuel grain.

Scale-up tests also confirm that this general theory is applicable to large-scale engines (Karabeyoglu et al., 2002c). Examples of ingredients that form a melt layer on the surface are normal alkanes such as methane, kerosene, paraffin waxes, PE waxes, and high-density polyethylene polymers.

Waxes with lower carbon chain lengths are characterized by lower melting temperature and lower viscosity, thus being more appropriate for increasing regression rates during combustion. On the other hand, branched waxes with higher carbon chain lengths have higher densities, thus increasing the system volumetric specific impulse. Branched waxes are characterized by lower shrinkage during solidification and have a higher melting point, thus being more suitable for applications with a wide temperature operational range. Moreover, two waxes from different suppliers that have identical melting points are not likely to possess the same properties because of the oil content and the processing method variability (Freund et al., 1982). Starting from previously obtained results (Toson et al., 2013; Kobald et al., 2013), experimental activity was performed on different waxes in terms of density measurements and mechanical properties. Moreover, experimental investigations were performed on microcrystalline wax-based mixtures consisting in thermal, rheological, and ballistic experiments performed at Politecnico di Milano, and viscosimetric tests performed at Space Propulsion Institute of DLR.

2. EXPERIMENTAL DETAILS

2.1 Density Measurements

A relatively new experimental facility was set up at the Aerospace Department of Politecnico di Milano, extended from a previous setup (Bradac, 2006). The experiment makes use of “a constant mass method.” A dilatometer is inserted in a controlled temperature water or oil bath. A measurement procedure was established and is reported here.

A dilatometer, made of a glass capillary tube and a glass bulb, is weighed and is found to have the resolution of 0.1 mg. An amount of solid paraffin, previously weighed, is inserted into the bulb, which is then put into an oven at a controlled temperature, thus allowing the paraffin to melt. The bulb is then extracted from the oven so the paraffin solidifies at an ambient temperature. This first step is necessary to avoid the presence of air bubbles trapped between the paraffin and the bulb, which would cause an erroneous paraffin volume reading.

After the paraffin solidification, a visual inspection of the presence of air bubbles is done and, if bubbles are present, the first step is repeated. The reference liquid is then inserted into the bulb and finally the capillary tube is pressed inside the conical part of the bulb (see Fig. 1). The overall system is weighed and inserted into a thermostatic bath for controlled heating. The use of a Phoenix 1 thermostat guarantees accuracy in

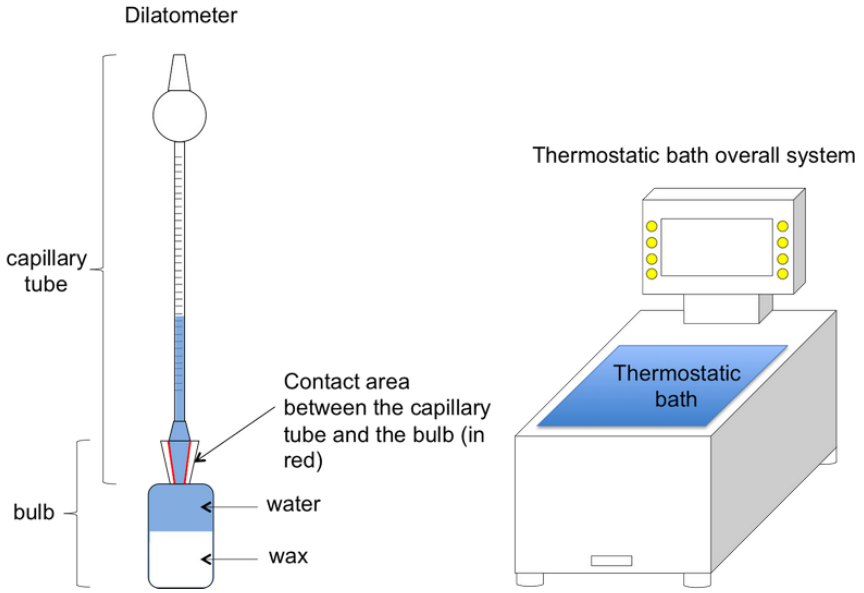

FIG. 1: Density measurement system (dilatometer and thermostatic bath not to scale). The dilatometer is inserted into the thermostatic bath.

temperature measurement of 0.01°C. Due to the low density of paraffin in its liquid state, water is selected as the reference liquid instead of mercury.

Starting from a temperature of 25°C, the volume variation of water and paraffin is measured by reading the graduated capillary of the dilatometer. When maximum capillary capacity is reached, some water has to be removed. After this step the system has to be reweighed and reinserted into the thermostatic bath.

Measurement is repeated at the desired temperature up to 90°C. For higher temperature measurements, a different material has to be considered both for the thermostatic bath and the reference liquid. The density of the reference liquid is fundamental because, if it is higher than the density of paraffin at its liquid state, it tends to settle below the paraffin, thus implying: (1) the paraffin will get into the capillary tube (thus making the reading of the volume unreliable because of its possible local solidification and consequent bubble formation after melting); (2) it is not possible to remove water from the capillary tube when the maximum capillary capacity is reached and (3) this results in a time-consuming cleaning process of the capillary tube after testing. The system conceptual design is given in Fig. 1.

2.2 Tensile Tests

Tensile tests were performed according to Standard ISO 527-1 using a MTS 858 machine on pure macroparaffin and microcrystalline wax, and on other mixtures, in order

to evaluate the effect of additives such as stearic acid and graphite. Mechanical uniaxial tests were performed at ambient temperature with two different velocities of the applied load, 0.5 and 5 mm/s. Elastic modulus, elongation, and maximum stress were calculated.

2.3 Experiments on Microcrystalline Mixtures

Experiments were performed on microcrystalline mixtures, which have a higher density, increased volumetric impulse, higher melting point, and softening temperature. With the aim to improve this last property, for applications where an extended temperature range is required, microcrystalline wax was mixed with a synthetic wax characterized by a melting point temperature higher than 100°C and a nominal low viscosity at high temperatures. Comparisons in terms of DSC thermal trace, rheological, and ballistic behavior were performed by experimental activity at Politecnico di Milano. DSC traces were obtained with a temperature scan of 10°C/min on 4-mg samples. Rheology experiments for storage modulus measurement were performed using a rotational plate-plate rheometer with 1% of applied constant strain and a shear rate sweep from 0.5 to 50 Hz. Regression rate tests were performed using the 2D radial microburner of SPLab in Politecnico di Milano (De Luca et al., 2006). Gaseous oxygen O_2 was used as an oxidizer. Tests were performed at a pressure of 16 bar and a 210 Nlpm oxidizer flow rate; quasi-steady operating conditions were reached, maintaining these parameters constant during the combustion. A data acquisition was made at 250 fps and at least 2 s of recording were considered for data postprocessing. The standard SPLab method for data reduction and ensemble average was used (De Luca et al., 2011).

Viscosity tests were performed at Space Propulsion Institute, DLR, Germany, using a parallel-plate rotational rheometer (HAAKE RheoStress 6000 rotational rheometer) with a plate diameter of 35 mm. Tests were performed at a constant temperature of 120°C and shear rates from 1 up to 3000 Hz.

3. EXPERIMENTAL RESULTS AND DISCUSSION

Tests were performed on different waxes, whose properties from the vendors are listed in Table 1. Stearic acid and graphite were also used as additives.

3.1 Density Measurement Results

Density values in the melting temperature range were deduced by measurements at solid and liquid states (Freund et al., 1982; Ukrainczyk et al., 2010). The instrumentation that was set up for this study allowed the measure of density, in solid-liquid phase transformation, to show a different curve slope. Preliminary results for pure microwax and macrowax are presented in Fig. 2 and Table 2, where the density percentage variation is presented as a function of the temperature. Density variation is referred to its initial value at 25°C.

TABLE 1: Paraffin properties from vendors

Wax ID	**Type**	**SP**	**CP**[a]	**DP**[b]	**Oil C**[c]	**Penetration**[d] **@ 25°C**	ν^{e} **@ 100°C**	ν^{f} **@ 120°C**
		[°C]	**[°C]**	**[°C]**	**[%]**	**[1/10mm]**	**[mm²/s]**	**[mm²/s]**
Wax 1	Paraffin wax	—	58–60	—	—	—	—	—
Wax 2	Paraffin wax	—	60–62	—	0–0.5	17–20	—	—
Wax 3	Paraffin wax	—	66–70	—	0–1	16–20	6–8	—
Wax 4	Paraffin wax	—	66–70	—	0–1	10–14	—	—
Micro	Microcrystal-line wax	—	83–94	88–102	0–2	4–10	—	8.5–12.5
Synth	Fischer-Tropsch hard wax	102–108	—	—	—	0–1	—	—

[a] Method ASTM D 938.
[b] Method Mettler 1°C/min.
[c] Method ASTM D 721.
[d] Method ASTM D 1321.
[e] Method ASTM D 156.
[f] Method ASTM D 445.

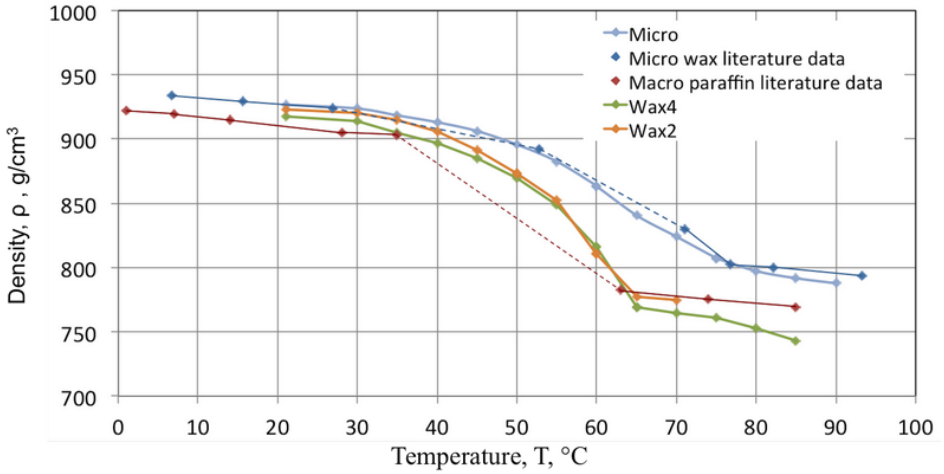

FIG. 2: Density curves as a function of temperature of wax 2, wax 4, and micro, and comparisons with literature data.

Density percentage variation from 25°C to 70°C for wax 2 and wax 4 is, respectively, 16% and 17%. As expected, the value is lower for micro, 11%, and it remains lower even if considering the last point of measure at 90°C. In general, the total expansion

TABLE 2: Density values at different temperatures

Temperature	**Density, ρ, kg/m^3**		
[°C]	**Wax 2**	**Wax 4**	**Micro**
25	923	918	927
30	920	914	924
35	915	905	918
40	906	897	913
45	891	885	906
50	873	870	896
55	852	848	883
60	811	816	864
65	777	769	841
70	775	765	824
75	—	761	807
80	—	753	797
85	—	743	792
90	—	—	788

of microcrystalline wax is lower than the total expansion of macroparaffin. The total smaller expansion of microcrystalline wax is associated to the absence of solid-phase transition (Freund et al., 1982). However, for a given commercial wax, the character of the relationship between specific volume and temperature depends not only on the carbon atom number and structure of the constituting individual alkanes, but also on the nature and amount of nonparaffinic compounds present in the wax that are a function of their production process.

Systematic error estimation, in the worst-case scenario, was done considering the following factors:

- Reading of graduated capillary. Considering a range of +/–0.5 mm, in the worst case the corresponding error in wax density calculation is +/–1 kg/m^3.
- Wax density measurement at reference temperature of 25°C. Considering the balance accuracy of 1 mg, the corresponding error in density calculation is lower than 1 kg/m^3 for all tested waxes.
- Expansion of the dilatometer. Knowing the linear coefficient of thermal expansion of dilatometer material, $\lambda = 9.5\text{E-}6\ \text{K}^{-1}$, the corresponding error in wax density calculation is negligible.
- Presence of air bubbles in the dilatometer bulb. Considering an overall bubbles volume associated to a +/–3.0 mm the reading of graduated capillary, the corresponding error in wax density calculation is +/–3 kg/m^3.

These factors introduce a total error in the worst-case scenario of +/– 3 kg/m^3.

3.2 Tensile Test Results

Tensile tests results are visible in Table 3. A comparison between a pure macroparaffin and a pure microcrystalline wax (Boiocchi et al., 2013), and the same waxes doped with stearic acid and graphite, is presented in terms of elastic modulus, maximum stress, and elongation percent. For every mixture and test condition, results are referred to the mean of at least eight tests.

As a result, at increasing velocities of applied load, the elastic modulus shows higher values for all tested waxes, as expected from the literature. Moreover, lower-melting-point waxes are characterized by a higher maximum tensile strength and larger percent elongation. The maximum stress standard deviation of microcrystalline wax is lower with respect to the corresponding macroparaffin, thus pointing out lower data scattering. The effect of additives is not so marked and brings an increase on the maximum stress value for tests performed at 0.5 mm/min and a decrease on the same value for tests performed at 5 mm/min. The main result of these tests is associated to the maximum stress values and the rupture typology of the samples: fragile rupture with maximum stresses between 1.74 and 2.38 MPa was measured for the microcrystalline wax, while ductile rupture was noticed for the macroparaffin, with maximum stresses between 2.21 and 3.03 MPa. The macroparaffin shows a clear elasto-plastic deformation, followed by a striction phase related to a localized deformation (see Fig. 3).

In order to not consider the elongation due to the possible slipping between the sample and the machine clamps in the measurements, an extensimeter was used. This was carefully inserted in the central zone of the restricted samples area (see Fig. 4).

It is necessary to point out that the ruptures were reached in the restricted samples area, but not all of them were reached in the zone between the two extensimeter hooks. This brings to a conservative result in terms of elongations.

TABLE 3: Tensile test results

Material	**Speed**	$E_{r,av}$	**SD**	σ_{max}	**SD**	**El**	**SD**
	[mm/min]	**[MPa]**	**[MPa]**	**[MPa]**	**[MPa]**	**[%]**	**[%]**
Wax 4	0.5	515.05	66.58	2.21	0.27	1.51	0.50
Wax 4	5	699.39	75.83	3.03	0.27	1.34	0.45
88% Wax 4 + 10% AS + 2% G	0.5	541.15	55.74	2.41	0.21	1.00	0.30
88% Wax 4 + 10% AS + 2% G	5	629.99	31.75	2.96	0.19	1.13	0.44
Micro	0.5	671.36	66.03	1.74	0.19	0.26	0.04
Micro	5	798.47	59.50	2.38	0.33	0.31	0.06
88% Micro + 10% AS + 2% G	0.5	622.29	45.65	1.81	0.52	0.31	0.11
88% Micro + 10% AS + 2% G	5	757.39	19.55	1.67	0.31	0.21	0.04

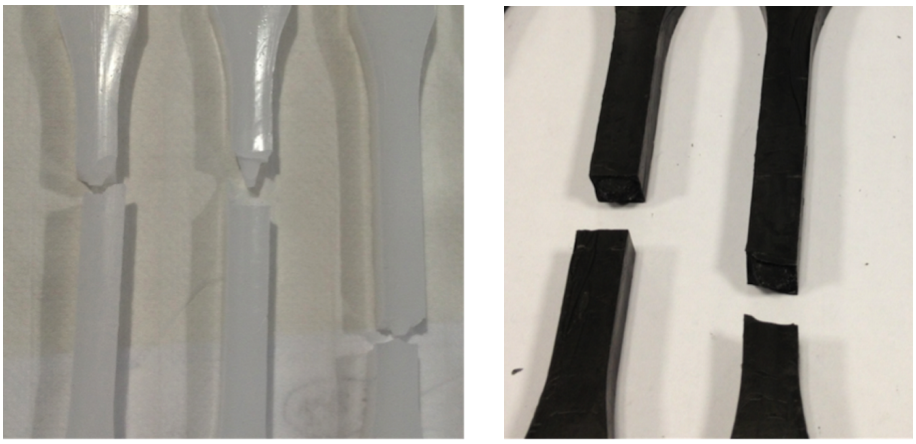

FIG. 3: Macroparaffin visible localized deformation. From the left: wax 4 and 88% wax 4 + 10% AS + 2% G.

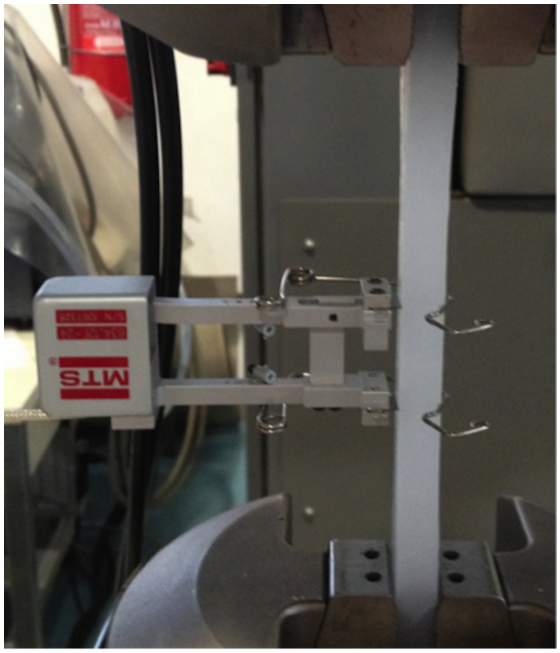

FIG. 4: MTS extensimeter inserted in a paraffin sample.

3.3 Experiments on Microcrystalline Wax Mixture Results

In order to increase the softening temperature of the mixtures without increasing viscosity, the stearic acid was substituted with a synthetic wax characterized by a higher nominal melting temperature. The main melting peak of this wax is presented in Fig. 5,

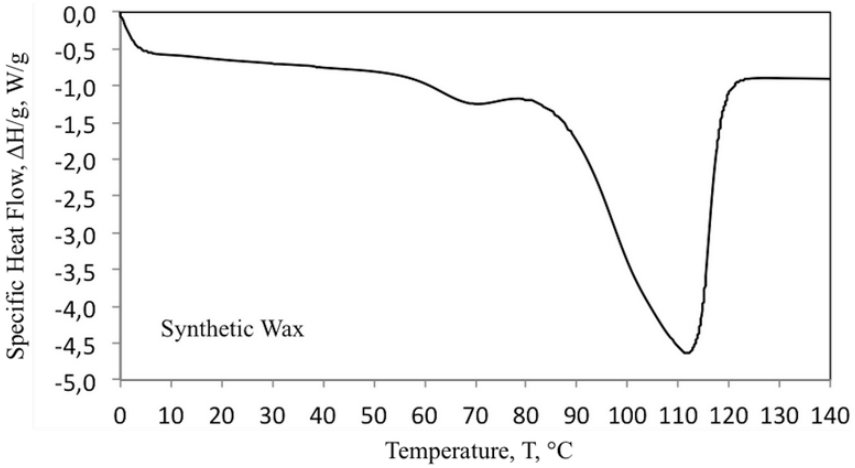

FIG. 5: Synthetic wax thermal behavior, DSC trace.

where the specific heat flow, which corresponds to the amount of heat absorbed during the transition divided by the sample mass, is presented in function of the temperature.

After verifying the miscibility goodness between microcrystalline wax “micro” and synthetic wax “synth,” DSC tests were performed on the microwax doped with stearic acid and graphite (88% micro + 10% AS + 2% G) and on the microwax doped with synthetic wax and graphite (88% micro + 10% synth + 2% G). Results show a sensible shift in the melting behavior, both in DSC temperature peaks and softening temperature (see Fig. 6). This is in agreement with the expectations, due to the synthetic wax higher melting temperature with respect to the stearic acid.

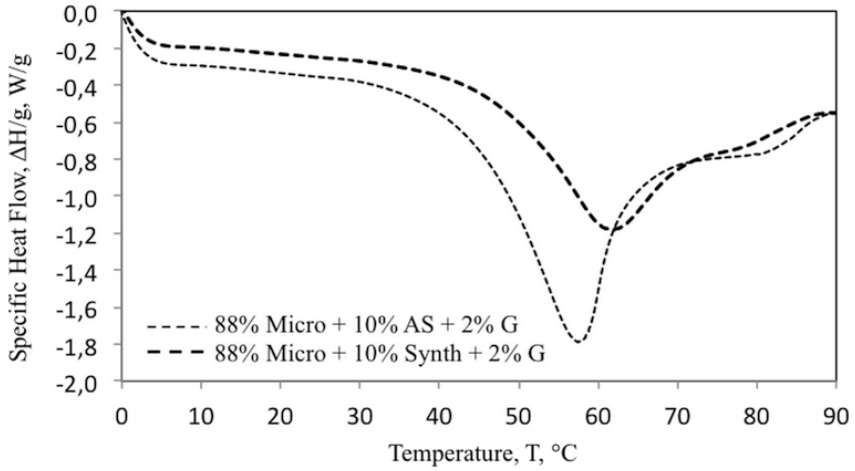

FIG. 6: DSC melting trace comparison between the microwax doped with stearic acid and graphite and the microwax doped with synthetic wax and graphite.

As a result of the rheological investigation, Fig. 7 shows that a higher storage modulus and an increase of 7°C in its preservation are reachable by the substitution of stearic acid with the synthetic wax.

The results of ballistic characterization are shown in Fig. 8, where the ensemble regression rate curves, with error bars, are presented as a function of the oxidizer mass flow rate. A pure HTPB ensemble regression rate curve is also presented as a reference

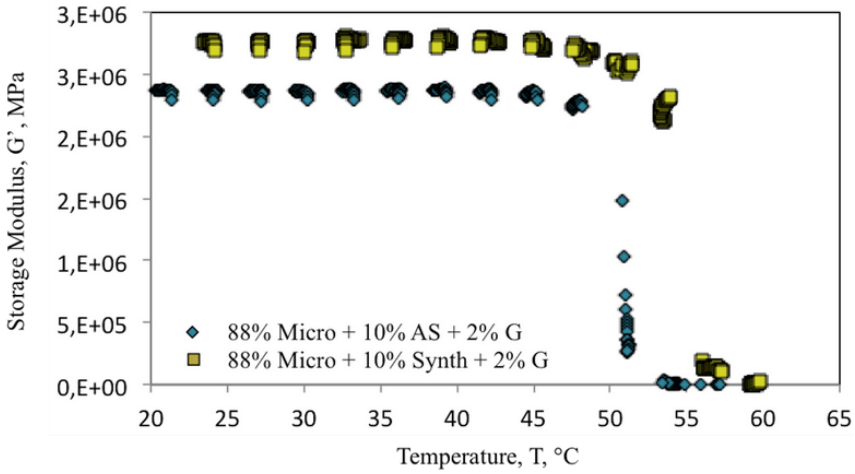

FIG. 7: Storage modulus comparison between the microwax doped with stearic acid and graphite and the microwax doped with synthetic wax and graphite.

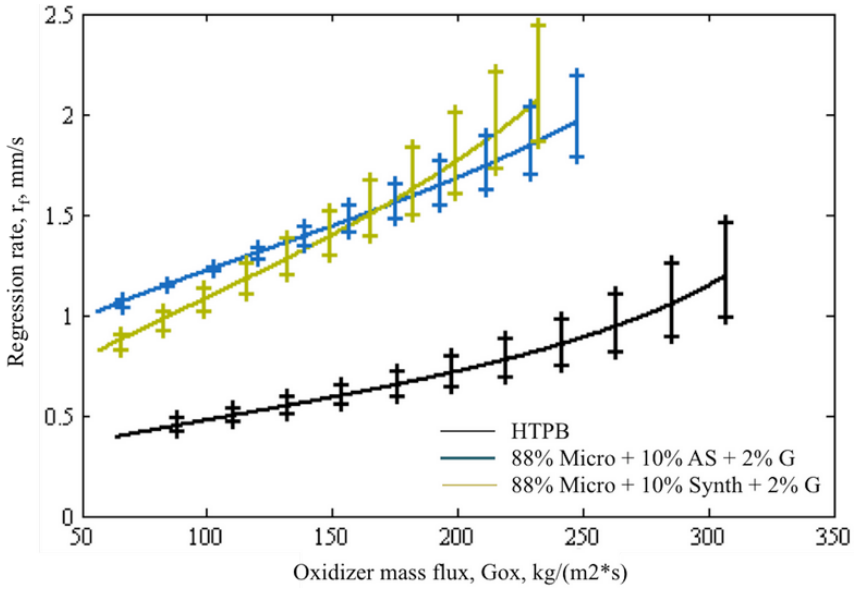

FIG. 8: Ensemble regression rate curves versus oxidizer mass flux.

for comparison purposes. (In this case tests were performed at 19 bar pressure.) Each ensemble curve was obtained from the interpolation of three to six single tests.

As a first result, a slightly higher sensibility on the oxidizer mass flow rate is appreciable on the microwax doped with synthetic wax. The mean regression rate percentage variations, for an oxidizer mass flow range from 120 kg/(m^{2}s) and 250 kg/(m^{2}s) were obtained using the following equation:

$$\text{percentage}\, r_f \text{ variation } = \frac{r_{f,\text{wax}} - r_{f,\text{HTPB}}}{r_{f,\text{HTPB}}} \times 100.$$

As in Table 4, there is no sensible difference in the regression rate mean value between the two paraffin-based mixtures. On the other hand, as expected, both mixtures have sensible higher regression rate values with respect to the HTPB baseline.

The regression rate for liquefying fuels is related to the fuel tendency to entrainment and consequently, as theorized by Karabeyoglu et al. (2002a), related to the melt layer viscosity by inverse proportionality. Therefore viscosity measurements have been performed at DLR Institute of Space Propulsion. The results presented in Fig. 9 show a lower viscosity for the mixture containing synthetic wax but maintaining, as expected, the same order of magnitude.

The viscosity measurements are in agreement with previous results (Toson et al., 2013) and confirm the regression rate results presented in Fig. 8.

4. CONCLUSIONS

An experimental characterization was performed on paraffin-based fuels which can be used for high regression rate applications in hybrid engines. The collected density data are useful for the preparation of solid fuel grains. They give a precise indication about the temperature ranges that have to be controlled in order to avoid the formation of internal tensile stresses during solidification. Tensile test data reveal that ductile rupture is reachable also for a pure paraffin having a melting temperature of 66–70°C, with maximum stress values up to 3 MPa.

The microparaffin test data reveal that improvements on softening point temperature are achievable by mixing with the synthetic wax. This solution causes a slightly lower

TABLE 4: Regression rate percentage variation with respect to HTPB baseline

Mixture	**Gox variation [%]**				
	120 [kg/m^{2}s]	**150 [kg/m^{2}s]**	**200 [kg/m^{2}s]**	**250 [kg/m^{2}s]**	**Mean**
HTPB baseline	—	—	—	—	—
88% micro + 10% AS + 2% G	152%	158%	169%	169%	162%
88% micro + 10% synth + 2% G	132%	150%	182%	196%	165%

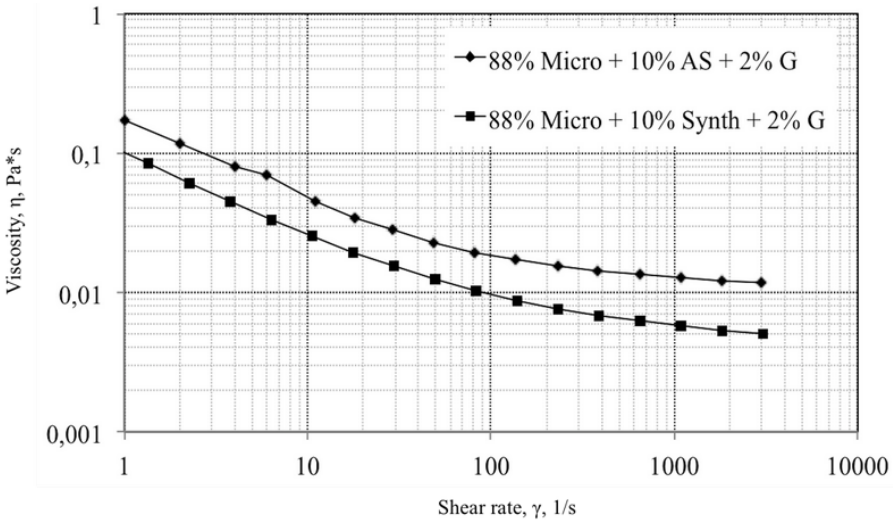

FIG. 9: Microwax doped with stearic acid and graphite and microwax doped with synthetic wax and graphite. Viscosity comparison at T = 120°C.

fuel viscosity and does not heavily affects the regression rate in the considered oxidizer mass flux range.

ACKNOWLEDGMENTS

The authors would like to thank Professor Daniele Pavarin of the University of Padua and his working group for their support, sharing experience, and paraffin procurement.

REFERENCES

Altman, A. and Holzman, A., Overview and history of hybrid rocket propulsion, *Fundamentals of Hybrid Rocket Combustion and Propulsion*, Chiaverini, M. J. and Kuo, K. K., Eds., Progress in Astronautics and Aeronautics, AIAA, Reston, VA, 2007.

Boardman, T. A., Hybrid propellant rockets, in Sutton, G. P. and Biblarz, O., Eds., *Rocket Propulsion Elements*, New York: Wiley, Ch. 15, pp. 579–607, 2001.

Boiocchi, M., Toson, E., Gelosa, S., Sliepcevich, A., Galfetti, L., and De Luca, L. T., Pure paraffin waxes analysis for hybrid rocket solid fuels: Rheological, thermal and mechanical characterization, *Proc. of the 5th European Conf. for Aeronautics and Space Sciences*, Munich, Germany, June 30–July 4, 2013.

Bradac, C., *Realizzazione, Calibrazione e Utilizzo di un Dilatometro per lo Studio Delle Proprieta' Termo-Volumetriche di Materiali Solidi e Liquidi*, MSc. Thesis, Politecnico di Milano, Milano, Italy, 2006.

De Luca, L. T., Hybrid rocket engines, in De Luca, L. T., Eds., *Energetic Problems in Aerospace Propulsion*, Milano, Ch. 12, pp. 1–92, 2009.

De Luca, L. T., Galfetti, L., Bosisio, F., Raina, H., Colombo, A., and Colombo, G., A hybrid micro-combustor for regression rate measurements, *Proc. of the 57th Intl. Astronautical Congress*, IAC-06-C4.2.01, Valencia, Spain, Oct. 2–6, 2006.

De Luca, L.T., Galfetti, L., Maggi, F., Colombo, G., Paravan, C., Reina, A., Tadini, P., Sossi, A., and Duranti, E., An optical time-resolved technique of solid fuels burning for hybrid rocket propulsion, in *The 47th AIAA/ASME/SAE/ASEE Joint Propulsion Conf. and Exhibit*, AIAA Paper no. 2011-5753, San Diego, CA, July 31–Aug. 3, 2011.

Freund, M., Csikos, R., Keszthelyi, S., and Mozes, G., *Paraffin Products, Properties, Technologies, Applications*, Amsterdam - Oxford - New York: Elsevier Scientific, pp. 94–102, 1982.

Karabeyoglu, M. A., Altman, D., and Cantwell, B. J., Combustion of liquefying hybrid propellants: Part 1, General theory, *J. Propul. Power*, vol. 18, no. 3, pp. 610–620, 2002a.

Karabeyoglu, M. A., Altman, D., and Cantwell, B. J., Combustion of liquefying hybrid propellants: Part 2, Stability of liquid films, *J. Propul. Power*, vol. 18, no. 3, pp 621–630, 2002b.

Karabeyoglu, M. A., Zilliac, G., Cantwell, B. J., De Zilwa, S., and Castellucci, P., Scale up tests of high regression rate liquefying hybrid rocket fuels, *J. Propul. Power*, vol. 20, no. 6, pp. 1037–1045, 2002c.

Kobald, M., Toson, E., Ciezki, H., Schlechtriem, S., Di Betta, S., Coppola, M., and DeLuca, L. T., Rheological, optical and ballistic investigations of paraffin-based fuels for hybrid rocket propulsion using a 2D slab-burner, *Proc. of the 5th European Conf. for Aeronautics and Space Sciences*, Munich, Germany, June 30–July 4, 2013.

Toson, E., Kobald, M., Di Betta, S., De Luca, L. T., Ciezki, H., and Schlechtriem, S., Rheological and ballistic investigations of paraffin-based fuels for hybrid rocket propulsion using a 2D radial micro-burner, *Proc. of the 5th European Conf. for Aeronautics and Space Sciences*, Munich, Germany, 2013.

Ukrainczyk, N., Kurajica, S., and Sipusic, J., Thermophysical comparison of five commercial paraffin waxes as latent heat storage materials, *Chem. Biochem. Eng. Q.*, vol. 24, no. 2, pp. 129–137, 2010.